Stark-Wannier states and Stark ladders in semiconductor superlattices

1989 J. Phys.: Condens. Matter 1 1449

(http://iopscience.iop.org/0953-8984/1/8/007)

J. Phys.: Condens. Matter **1** (1989) 1449–1466. Printed in the UK

Stark–Wannier states and Stark ladders in semiconductor superlattices

J Leo† and A MacKinnon
The Blackett Laboratory, Imperial College, London SW7 2BZ, UK

Received 30 June 1988, in final form 26 September 1988

Abstract. A two-band tight-binding Hamiltonian is used to investigate the interaction between the energy bands of a periodic system in the presence of an electric field. Information on the existence of Stark–Wannier states and Stark ladders in this two-band system is obtained. The possibility of using a semiconductor superlattice device to experimentally observe Stark ladders and Zener tunnelling between the energy bands is also discussed.

1. Introduction

The effect of a substantial electric field applied across a periodic structure was first investigated by Zener [1] who used the sloping band picture (figure 1) to study electrical breakdown in solids caused by electrons crossing from the valence band to the conduction band, an effect now termed Zener tunnelling. The concept of a Stark ladder was later introduced by Wannier [2, 3] to explain the energy spectrum of states within these sloping bands. It is derived by writing the Schrödinger equation for the periodic system in the presence of an applied electric field as

$$\left(\frac{p^2}{2m^*} + V(x) - eFx\right)\Psi(x) = E\Psi(x). \tag{1}$$

As $V(x + a) = V(x)$, a translation of (1) by a lattice constant 'a', gives

$$\left(\frac{p^2}{2m^*} + V(x) - eFx\right)\Psi(x + a) = (E + eFa)\Psi(x + a) \tag{2}$$

Therefore, for any state located at an energy E, there is an identical state located at a shifted energy $E + eFa$ with the same wavefunction except that its position is displaced by a lattice constant. In fact (1) can be translated by any number of lattice constants to eventually form the familiar Stark ladder given by

$$E_m = eFam + E_0 \tag{3}$$

where m labels the Stark state and E_0 denotes the origin of the ladder.

Therefore, the basic requirement exists that every energy level must belong to a ladder and that the states of the ladder are spatially shifted relative to one another by

† Present address: Max-Planck-Institut Für Festkörperforschung, Heisenbergstrasse 1, D-7000 Stuttgart 80, Federal Republic of Germany.

0953-8984/89/081449 + 18 $02.50

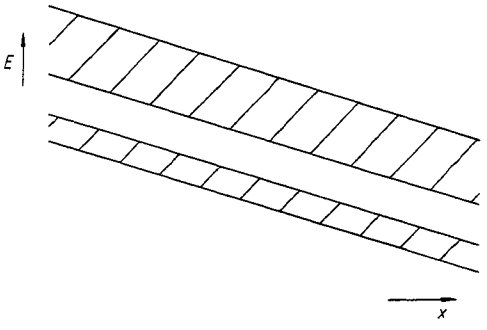

Figure 1. Energy versus position diagram showing the effect an electric field has on the bands of a periodic system. The shaded areas represent the allowed energy regions.

integer multiples of the lattice constant. In fact, we will show later that there is a one-to-one relationship between each state in the ladder and each unit cell. It is not required, however, that every energy level must belong to the same ladder. Indeed this can not always be possible if the above requirements are to be satisfied. In a system with only one energy band, all the Stark levels will belong to the same ladder. The inclusion of an extra band will result in another Stark ladder being formed to incorporate the extra energy levels. In the context of the sloping band picture, we can view each band as being comprised of a Stark ladder of energy states.

To understand how these banded Stark ladders interact with each other, we shall now study in more detail the Schrödinger equation given in (1). We write the Stark–Wannier wavefunctions as superpositions of Bloch states

$$\Psi(x) = \sum_{n',k'} C(n', k')|n', k'\rangle. \tag{4}$$

Substituting (4) into (1) and multiplying through by the Bloch state $\langle n, k|$ gives

$$[\varepsilon(n, k) - E]C(n, k) = eF \sum_{n',k'} \langle n, k|x|n', k'\rangle C(n', k') \tag{5}$$

where $\varepsilon(n, k)$ is the Bloch energy. The matrix element can now be written [4]

$$\langle n, k|x|n', k'\rangle = \mathrm{i}\delta_{n,n'}\delta_{k,k'}\frac{\partial}{\partial k} + \delta_{k,k'}X_{n,n'} \tag{6}$$

where

$$X_{n,n'} = \mathrm{i}N\int_0^a \mathrm{e}^{\mathrm{i}(k'-k)x} u^*_{nk}(x)\frac{\partial}{\partial k}u_{n'k'}(x)\,\mathrm{d}x \tag{7}$$

$u_{nk}(x)$ is the periodic part of the Bloch function and the integral is only over a unit cell.

The effective Schrödinger equation now has the form

$$[\varepsilon(n, k) - E]C(n, k) = \mathrm{i}eF\frac{\partial}{\partial k}C(n, k) + eF\sum_{n'} X_{n,n'}C(n', k). \tag{8}$$

The important term here is the matrix element $X_{n,n'}$ which couples the bands together. In the paper by Saitoh [4], this term was neglected to enable a study of a single band

system to be made. Using the tight-binding approximation, Saitoh derived the Stark–Wannier wavefunction to be

$$\Psi(x) = \frac{1}{\sqrt{a}} J_{x/a-m}\left(\frac{W/2}{eFa}\right) \tag{9}$$

where $J_n(x)$ is the Bessel function of the first kind and W is the band width. This now shows that an electron in the mth state of the single-band Stark ladder is centred around $x = ma$, and localised within a length W/eF called the Stark length L_s. The zero-point energy of the Stark ladder E_0 was also derived for the single band model and found to be

$$E_0 = \frac{a}{2\pi}\int_{-\pi/a}^{\pi/a} \varepsilon(k)\,\mathrm{d}k \tag{10}$$

where $\varepsilon(k)$ is the dispersion relation for the unperturbed system.

In order to carry out a complete multiband analysis, it is important to include the interband term $X_{n,n'}$ when solving (8) to allow for Zener tunnelling between bands. This then permits the delocalisation of electrons. However, there has been some controversy about whether this matrix element between the bands actually exists [5–7]. Fukuyama *et al* [8] have studied this problem briefly using a two-band model and have concluded that two interpenetrating Stark ladders do exist and that they are coupled together. This is a very important point as an absence of any interband coupling could dramatically reduce the transport of electrons through the system.

Emin and Hart [9] have attempted to solve the problem of a multiband system analytically. They divide the effect of an electric field on a one-dimensional chain of N square-well potentials in the presence of an electric field into two components. One component alters the shape of each potential well whilst the other shifts each one by an energy eFa relative to its neighbour ('a' is still the period). The first effect can then be included into the system's periodic potential to form a basis of electric-field-dependent Bloch states and the second effect can be represented by a step function in the Hamiltonian. The matrix element given in (5) can be rewritten in the following way to represent the effect splitting the field into the two components has on the interband coupling.

$$\begin{aligned}\langle n, k|x|n', k'\rangle &= \int_0^{Na} \mathrm{e}^{\mathrm{i}(k'-k)x} u^*_{nk}(x)\, x\, u_{n'k'}(x)\,\mathrm{d}x \\ &= \sum_{m=0}^{N-1} \mathrm{e}^{\mathrm{i}(k'-k)ma}\int_0^a \mathrm{e}^{\mathrm{i}(k'-k)x} u^*_{nk}(x)\, x\, u_{n'k'}(x)\,\mathrm{d}x \\ &\quad + \sum_{m=0}^{N-1} ma\mathrm{e}^{\mathrm{i}(k'-k)ma}\int_0^a \mathrm{e}^{\mathrm{i}(k'-k)x} u^*_{nk}(x) u_{n'k'}(x)\;\mathrm{d}x\end{aligned} \tag{11}$$

As we are considering a *finite* system we can write

$$\sum_{m=0}^{N-1} \mathrm{e}^{\mathrm{i}(k'-k)ma} = N\delta_{k,k'} \tag{12}$$

as an exact relation for the ks that satisfy

$$k = 2\pi/Nan \qquad \text{where } n \text{ is an integer} \tag{13}$$

The ks therefore form a complete representation of the finite system. Where necessary,

(12) should be treated as the definition of the Kronecker delta. The matrix element can now be written

$$\langle n, k|x|n', k'\rangle = N\delta_{k,k'} \int_0^a u_{nk}^*(x)\, x\, u_{n'k'}(x)\, \mathrm{d}x - \mathrm{i}N \frac{\partial}{\partial k'} (\delta_{k,k'}) I(n, k; n', k') \tag{14}$$

where

$$I(n, k; n', k') = \int_0^a \mathrm{e}^{\mathrm{i}(k'-k)x} u_{nk}^*(x) u_{n'k'}(x)\, \mathrm{d}x. \tag{15}$$

The first term in (14) contains the component of the field that alters the shape of the wells and the second term results from the step-function potential which shifts each well relative to its neighbour. The second term can be written in the following way:

$$iN\left(\delta_{k,k'} \frac{\partial}{\partial k'} I(n,k;n',k') - \frac{\partial}{\partial k'}[\delta_{k,k'} I(n,k;n',k')]\right). \tag{16}$$

Emin and Hart then show that after summing over k' and n', the first term is zero and the second gives no interband coupling. They therefore conclude that it is the effect of the electric field on the shape of the wells that gives the interband coupling.

To continue the work on a multiband system, a two band tight-binding Hamiltonian will be used to study the properties of a one dimensional periodic system 50 units long in the presence of an electric field. A two-band model is used as it contains all the essential physics of interband coupling without the problems associated with a complete multiband analysis. The use of more than two bands would just make the situation more complicated without introducing any new concepts. We will clarify some of the aspects in the theory of Stark–Wannier states and Stark ladders by solving the model numerically and show how the energy bands interact with one another. We will also show that Emin and Hart are mistaken in the way they consider the bands to interact. We will also describe how to observe the effects of the Stark ladders and show that this can best be done using a superlattice structure.

2. The model

To explicitly calculate the energy spectrum and the wavefunctions of a periodic two-band system in the presence of an electric field, we use a one-dimensional nearest-neighbour tight-binding model. We define two states on site i, an s state $|i, \mathrm{s}\rangle$ and a p state $|i, \mathrm{p}\rangle$ which are both tightly bound onto that site. We therefore write the Hamiltonian representing a two-band system as

$$\begin{aligned} H = {} & \sum_i \varepsilon_s |i,\mathrm{s}\rangle\langle \mathrm{s},i| - V_s(|i-1,\mathrm{s}\rangle\langle \mathrm{s},i| + |i,\mathrm{s}\rangle\langle \mathrm{s},i+1|) \\ & + \sum_i \varepsilon_p |i,\mathrm{p}\rangle\langle \mathrm{p},i| - V_p(|i-1,\mathrm{p}\rangle\langle \mathrm{p},i| + |i,\mathrm{p}\rangle\langle \mathrm{p},i+1|) \\ & + \sum_i V_{sp}(|i-1,\mathrm{s}\rangle\langle \mathrm{p},i| + |i,\mathrm{s}\rangle\langle \mathrm{p},i+1|) \\ & - \sum_i V_{sp}(|i-1,\mathrm{p}\rangle\langle \mathrm{s},i| + |i,\mathrm{p}\rangle\langle \mathrm{s},i+1|) \end{aligned} \tag{17}$$

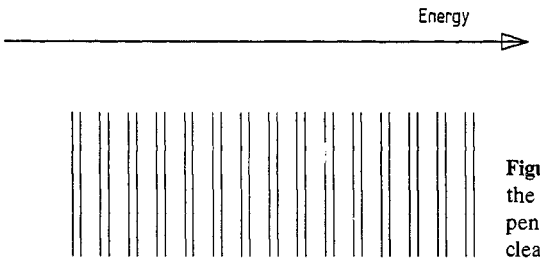

Figure 2. The energy spectrum of the two-band model. Two interpenetrating Stark ladders are clearly visible.

where ε_s and ε_p correspond to the on-site energies of the s and p orbitals, V_s and V_p correspond to the matrix element between s and p orbitals respectively and V_{sp} is the matrix element between an s orbital and its neighbouring p orbital.

To form two bands where the second band is wider than the first and the gap between them is of the order of the band widths we used $\varepsilon_s = 0$, $\varepsilon_p = 14$, $V_s = 1$, $V_p = 3$ and $V_{sp} = 2$. This results in the width of the lower band, which we shall refer to as the s band, being 4 and the width of the upper band, the p band, being 12. The resulting band gap was 6. To simulate the effect of the electric field we perturbed each on-site energy by eFi where e is the electronic charge which was set to one, F the field strength and i the site label. This is known as the ladder approximation. Although we refer to the two bands as s bands and p bands, these bands are never comprised of states that are purely s-like or p-like, but of a mixture. Of course, in the absence of an electric field, the s band does contain more s-like states than p-like states and similarly for the p band.

3. Results

Figure 2 is an energy level diagram obtained by diagonalising the Hamiltonian given in (17) at $F = 1.265$. The two interpenetrating Stark ladders are clearly discernible and the spacing between the energy levels in each of the ladders is eFa. This is therefore in total agreement with the result obtained by Fukuyama *et al* [8]. It should be noted here that the energy levels given in figure 2 are only a selection which represent the energy spectrum in the bulk material. Energy levels that lie at the extremes of this energy spectrum are effected by the edges of the sample. This consequently results in a modification of the energy spacing between the Stark levels.

To confirm the validity of viewing the Stark ladders as belonging to separate bands, we calculated the wavefunction of two neighbouring energy states, each one belonging to one of the ladders given in figure 2 (cf figure 3). It can clearly be seen that each wavefunction has its maximum centred on different points. By referring back to figure 1, we can see that a state which belongs to one of the bands has its centre or its point of maximum amplitude shifted relative to a state that belongs to the other band. Therefore, from figure 3 we conclude that the wavefunctions, and therefore the Stark ladders, do belong to different bands.

Furthermore, let us also consider the spatial extent of the wavefunction. In figure 3 each wavefunction covers about 20 sites. The Stark length at a field of 1.265 and with a band width of 22 (this includes both bands and the gap) is 17.4. It therefore seems that the wavefunctions straddle both bands. But it is also clear in figure 3 that the wavefunction

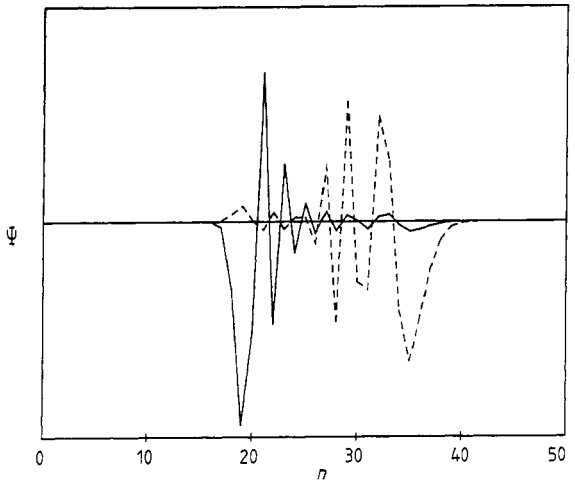

Figure 3. Two Stark–Wannier wavefunctions at $F = 1.236$. Notice how their centres are spatially shifted relative to one another.

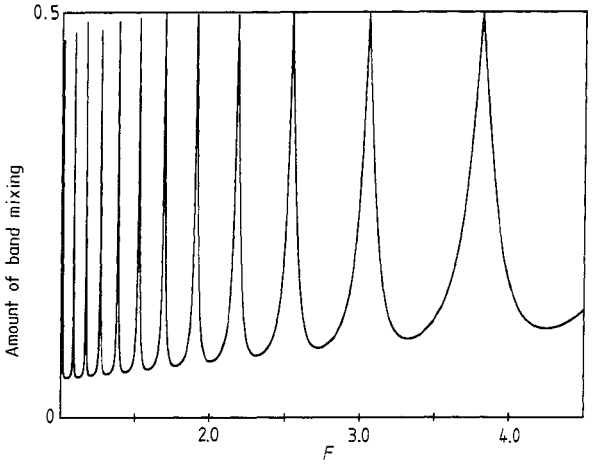

Figure 4. The amount of p state in a wavefunction belonging to the lower band plotted against varying electric field.

represented by a dotted curve has a longer allowed energy region than its counterpart which points to it having a longer Stark length. We therefore conclude that this wavefunction must belong to the wider band (the p band).

From the way the wavefunctions straddle both bands, it seems evident that there must be tunnelling between the bands at this field and therefore, there must be some mixing of states belonging to different ladders. By varying the field it is possible to vary the relative position of the ladders which must effect the mixing of states belonging to different bands. Furthermore, when the ladders exactly line up and become degenerate with one another, each wavefunction must have an equal component of states belonging to both the s band and the p band. We therefore plot the amount of p state in a wavefunction belonging to the s band versus field (figure 4) to give an indication of the amount of band mixing at different fields. Every peak in the graph indicates a degeneracy

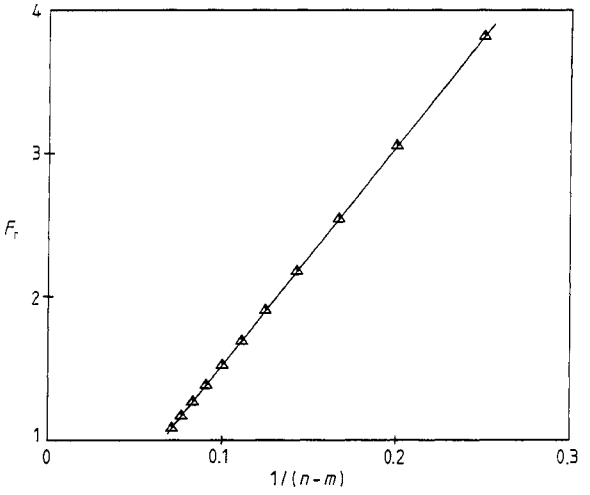

Figure 5. Plot of the electric field at which resonance occurs between the two bands against the reciprocal of the Stark ladder indexes.

in energy resulting from the two ladders resonating with each other. This seems to become less frequent however as the field is increased and is certainly not periodic.

The field at which the resonances occur F_r, can be found by using (3). We label the states in the lower band as E_n, and for the upper band we use E_m. At resonance, $E_m = E_n$, which gives

$$F_r = \frac{E_p - E_s}{ea(n-m)} \tag{18}$$

where E_p is the zero point of energy for the upper band and E_s is that for the lower band. So resonance between the Stark ladders occurs at a field given by the reciprocal of integer numbers ranging from 1 to 49. That is the first resonance occurs when the first Stark state from the p band ($m = 1$) lines up with the 50th Stark states from the s band ($n = 50$). The second resonance will then occur when the second Stark state from the p band ($m = 2$) lines up with the 50th Stark states from the s band ($n = 50$). This is equivalent to the first Stark state from the p band ($m = 1$) lining up with the 49th Stark state from the s band ($n = 49$).

For a one-band model Saitoh derived (10) to give the zero-point energy, which for the tight-binding model is $E_p - E_s = \varepsilon_p - \varepsilon_s$ as the integral of $\cos ka(\varepsilon(k) = \varepsilon - 2V \cos ka)$ over the Brillouin zone is zero. Therefore, $E_p - E_s = 14$. By plotting F_r versus $1/(n-m)$ (figure 5) for our model we find that the points completely lie on a straight line with a gradient of 15.29 ± 0.05. For $a = e = 1$, equation (18) gives a gradient of 14. This small discrepancy in the gradient is due to the fact that the values used for E_p and E_s in (18) are only valid for a one-band model. For two interacting bands we can expect $E_p - E_s$ to be somewhat larger.

When the two Stark ladders are in resonance, the Stark–Wannier states in the two bands are degenerate. If there is a non-zero matrix element between the bands then we can expect this degeneracy to be lifted by each pair of Stark–Wannier states splitting and consequently anticrossing as the field is varied. In figure 6 we follow two levels, each located in different bands, as the field is varied. If there was a zero matrix element between the bands so that Zener tunnelling did not take place, then the levels would

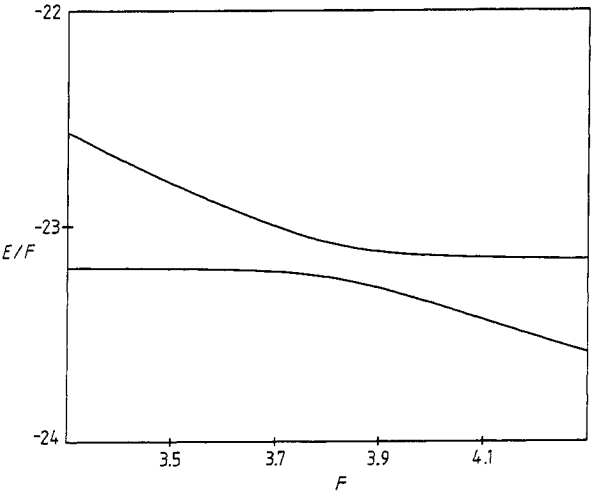

Figure 6. Anticrossing of energy levels belonging to different Stark ladders. This represents a movement of charge between the bands.

cross, but it is very clear that they do not cross. This means that if an electron is located in the lower band, it will cross over to the upper band as the field is varied.

To follow the form of the wavefunction as this happens it is useful to plot the inverse participation ratio P^{-1} which was first introduced by Bell and Dean [10] in the theory of localisation. It is defined as

$$P^{-1} = \sum_i |\Phi_i|^4 \Big/ \left(\sum_i |\Phi_i|^2\right)^2 \tag{19}$$

where Φ_i is the amplitude of the wavefunction on site i. It is effectively a measure of the volume occupied by the wavefunction and can be used as a means of finding the extent of the wavefunction. For example, if it is becoming more extended, P^{-1} will tend to zero as the dominator in (19) dominates over the numerator. However, if the wavefunction is becoming more localised P^{-1} will tend to a constant. Therefore when there is maximum band mixing in our model, the wavefunction is at its maximum extension. This is shown in figure 7. Alignment between the two ladders causes a large dip in P^{-1} characterising delocalisation. It should also be noted that P^{-1} is getting larger at maximum misalignment as the field is increased. This means that when the wavefunctions are centred on their respective bands, they are becoming more localised. This is in agreement with the fact that the Stark length depends on the inverse of the field ($L_s = W/eF$).

4. Zener tunnelling

The size of the anticrossing of the energy levels can be a useful quantity to know when the size of the tunnel current that is flowing between the two bands is needed. In fact it is a very relevant quantity for characterising the amount of band mixing. Figure 4 is a useful plot for finding the field at which resonance occurs between the two bands, but it does not convey any information about how strong the resonance is. Consequently, we plot the size of this anticrossing Δ against the field (figure 8). Δ clearly increases as the field is increased with the gradient getting steeper as the field gets higher.

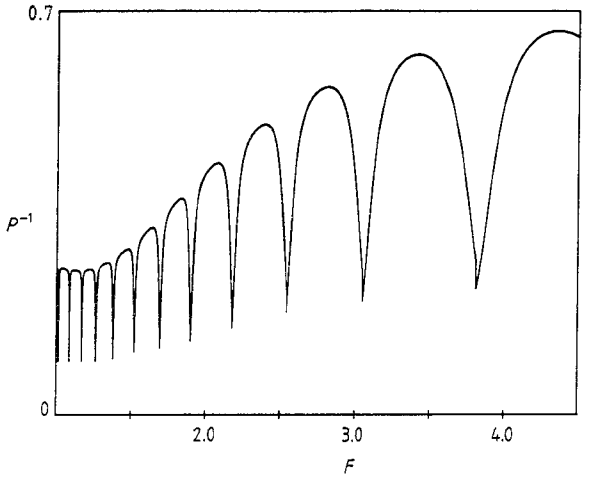

Figure 7. The inverse participation ratio plotted against the electric field. Notice that P^{-1} is increasing on average. This represents the electron becoming increasingly localised.

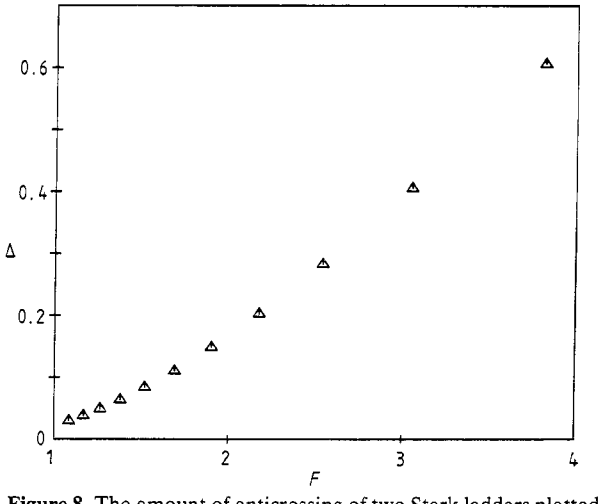

Figure 8. The amount of anticrossing of two Stark ladders plotted against the electric field.

It may be argued that the interband coupling is a result of surface effects as we are only considering a finite system. However, because an increase in the field results in a decrease in the Stark length, the bulk Stark states interact less with the edges at larger fields. Therefore the amount of interband mixing should decrease as the field increases. As this is not observed, it can be concluded that the interband coupling is not a result of surface effects.

The increase in Δ may be understood in the following way. The distance between the bands, which is given by E_g/eF, is decreasing as the field is increasing. Therefore, the overlap between the two bands is increasing resulting in a larger splitting of the energy levels. An alternative way of viewing this is that at the lower fields, the two levels that resonate have wavefunctions situated on sites that are fairly widely separated. However, resonances that occur at high fields are between states that are spatially much nearer.

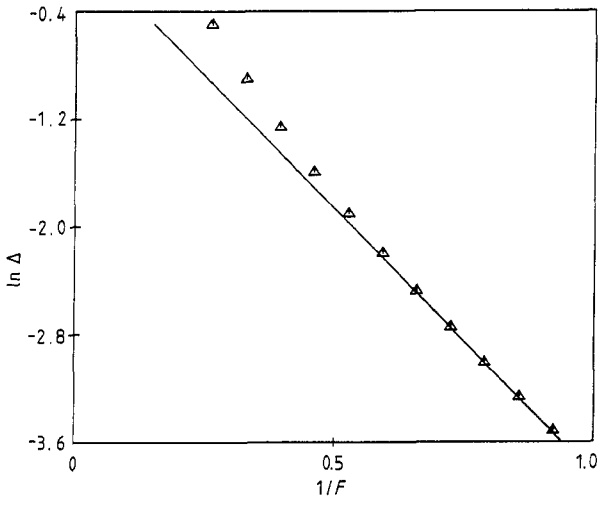

Figure 9. The natural logarithm of the amount of anticrossing of the two Stark ladders plotted against the reciprocal of the electric field.

To find a form for Δ as a function of field we construct the following argument. Using the uncertainty principle we expect the tunnelling time τ to be given by

$$\tau \simeq \hbar/\Delta. \tag{20}$$

Therefore the tunnelling rate Γ, which is equal to the reciprocal of the tunnelling time goes as

$$\Gamma \simeq \Delta. \tag{21}$$

At this point we can make an estimate of the tunnelling time between bands using the above equation. Taking a value for Δ from figure 8 of 0.2 and translating it into realistic units gives a value of 2 meV. This results in a tunnelling time of about 3×10^{-13} s. From the WKB approximation, the rate Γ is given by

$$\Gamma \simeq \exp\left[-2\int_b^a k \, \mathrm{d}x\right] \tag{22}$$

where $k^2 = 2m^*/\hbar^2\,(V(x) - E)$. From figure 1, we can view the band gap as forming a triangular barrier where

$$V(x) = E_g - eFx. \tag{23}$$

This gives

$$\Gamma \simeq \exp\left(\frac{-4(2m^*)^{1/2}}{3\hbar}\frac{E_g^{3/2}}{eF}\right). \tag{24}$$

Combining (21) and (24) gives

$$\Delta \simeq \exp\left(\frac{-4(2m^*)^{1/2}}{3\hbar}\frac{E_g^{3/2}}{eF}\right). \tag{25}$$

Therefore a plot of ln Δ against $1/F$ should result in a straight line of negative gradient. Figure 9 is just such a plot of our data and exhibits a fairly good straight line, especially

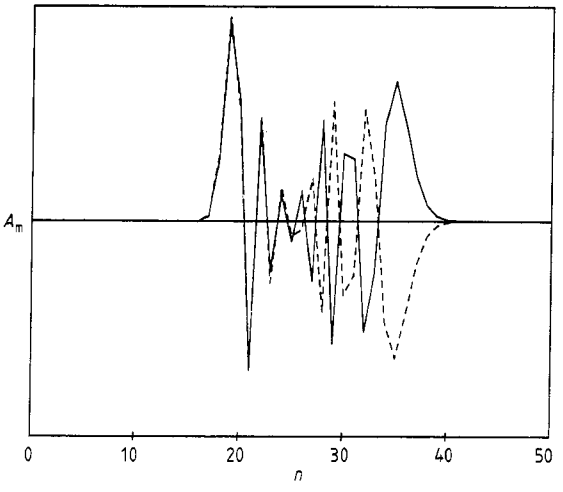

Figure 10. Two Stark–Wannier wavefunctions plotted at resonance. The wavefunctions seem to be superpositions of the single band states.

at lower fields. It is at the higher fields when one would expect the above theory to break down. This is because (25) is derived on the assumption that the wavefunctions are plane waves either side of the barrier and that the height of the potential barrier varies slowly in space. Both of these conditions are clearly violated at large electric fields.

It would now seem from this analysis that equations (24) and (25) do at least give an approximate form for the variation of the rate of tunnelling across the two bands as a function of the field. So instead of having the rather counter-intuitive result that increasing the electric field localises the electrons, as is obtained in the single-band picture, we do indeed find that the electric field does increase the current across the sample, albeit only at the points of resonance between the bands. But these resonances are very closely spaced at very low fields and it would not take much broadening attributable to some scattering mechanism to smear all these peaks out.

5. Multiband Stark–Wannier states

We shall now concentrate on the form of the Stark–Wannier states. This will allow a comparison to be made with the one obtained analytically by Saitoh in the single band model (equation (9)). Figure 10 is a plot of the Stark–Wannier wavefunctions when the two bands are at resonance (i.e., the two wavefunctions represent the two energy states given in figure 6 when they are at maximum anticrossing). It is clear from this plot that the resultant wavefunctions are linear combinations of two states, each one centred on and belonging to each band. The wavefunction represented by a continuous line, $A_m^1(x)$ is therefore given by

$$A_m^1(x) = |1\rangle + |2\rangle \tag{26}$$

whilst $A_m^2(x)$ which is represented by the broken curve is given by

$$A_m^2(x) = |1\rangle - |2\rangle \tag{27}$$

The form for the states $|1\rangle$ and $|2\rangle$ also closely resemble the Bessel function solutions

for the single band case. We therefore conclude that the Stark–Wannier states for a multiple-band system are simply a superposition of the single band states which are Bessel functions of the first kind.

As we are studying a tight-binding model, the field has no effect on the individual sites. Therefore, in the language of Emin and Hart, we are effectively only considering the step-function potential in the Hamiltonian and this gives no interband coupling. However, as we have shown, we do indeed get interband mixing using this model. To investigate this, we shall study the interband matrix element $\langle n, k|x|n', k'\rangle$ for the two band tight-binding model of finite length. The basis functions $|n, k\rangle$ are now given by

$$|n, k\rangle = e^{ikpa}[S_{n,k}|s\rangle + P_{n,k}|p\rangle] \tag{28}$$

on each site. S is the s-like function and P is the p-like function which both depend on the wavevector k and the band index n. Following Emin and Hart, the x in the matrix element is replaced by the step function

$$\begin{aligned} S(x) &= 0 \qquad \text{for} \qquad x < 1 \\ S(x) &= 1 \qquad \text{for} \qquad x \geqslant 1 \end{aligned} \tag{29}$$

to give

$$\begin{aligned} &\langle n, k|\sum_{m=1}^{N} S(x/a - m)|n', k'\rangle \\ &\quad = \int_0^{Na} [\langle s|S^*_{n,k} + \langle p|P^*_{n,k}]\sum_{m=1}^{N} S(x/a - m)[S_{n',k'}|s\rangle + P_{n',k'}|p\rangle]\, e^{i(k'-k)pa}\, dx \\ &\quad = \sum_{p=1}^{N} p\, e^{i(k'-k)pa}\int_0^a [\langle s|S^*_{n,k} + \langle p|P^*_{n,k}][S_{n',k}|s\rangle + P_{n',k'}|p\rangle]\, dx \\ &\quad = -i\frac{N}{a}\frac{\partial}{\partial k'}(\delta_{k,k'})I(n, k; n', k'). \end{aligned} \tag{30}$$

Again we have made use of the relation given in (12). Equation (30), not surprisingly, has the same form as the second term in (14), but with a different $I(n, k; n', k')$. If we substitute this back into the Schrödinger equation given in (5), we get

$$\begin{aligned} [\varepsilon(n, k) - E]C(n, k) &= -ieFN\sum_{n',k'}\frac{\partial}{\partial k'}(\delta_{k,k'})I(n, k; n', k')C(n', k') \\ &= ieFN\sum_{n',k'}\delta_{k,k'}\frac{\partial}{\partial k'}(I(n, k; n', k')C(n', k')) \\ &= ieFN\left(\frac{\partial}{\partial k}C(n, k) + \sum_{n',k'}\delta_{k,k'}C(n', k')\frac{\partial}{\partial k'}I(n, k; n', k')\right) \end{aligned} \tag{31}$$

where we have used the relation [9]

$$\delta_{k,k'}I(n, k; n', k') = \delta_{n,n'}\delta_{k,k'} \tag{32}$$

to obtain the first term in (31) above and we have used the fact that

$$\sum_{k'}\frac{\partial}{\partial k'}(I(n, k; n', k')C(n', k')\delta_{k,k'}) = 0. \tag{33}$$

This is because the function being differentiated is a periodic function of k'. It is also

quite justified to have a discrete set of k's and a continuous derivative in (33). This point is shown to be true in Appendix 1 for a general periodic function of k'.

It should also be mentioned here that $\varepsilon(n, k)$ in (31) is not strictly the Bloch energy. It does include extra terms because we are dealing with a finite system. However, these terms are not important and are certainly not the cause of the interband coupling because of the following argument. Increasing the length of the system is equivalent to increasing the field as this reduces the Stark length which in turn reduces the coupling between the Stark states and the edges. If the interband coupling was due to the boundaries and the length of the system was increased (i.e., the field was increased) the extra boundary terms in $\varepsilon(n, k)$ would become smaller and so the amount of band mixing should decrease. However, as we have shown through our numerical work and our arguments an increase in the field results in more band coupling. Consequently this inconsistency means that $\varepsilon(n, k)$ can not be responsible for interband coupling and so for the purposes of the present work these extra terms can be ignored.

The derivative of $I(n, k; n', k')$ with respect to k' can be written

$$\delta_{k,k'} \frac{\partial}{\partial k'} I(n, k; n', k')$$

$$= \delta_{k,k'} \int_0^a [\langle s|S^*_{n,k} + \langle p|P^*_{n,k}] \frac{\partial}{\partial k'} [S_{n',k'}|s\rangle + P_{n',k'}|p\rangle] \, dx. \tag{34}$$

This is the important term which couples the bands and cannot be zero unless the S and P functions are independent of k. This is because $[S_{n',k}|s\rangle + P_{n',k}|p\rangle]$ is orthonormal to $[S_{n,k}|s\rangle + P_{n,k}|p\rangle]$ for $n \neq n'$. Therefore these can be viewed as two perpendicular vectors in a two-dimensional space lying on a unit circle. Consequently, the derivative with respect to k of $[S_{n',k}|s\rangle + P_{n',k}|p\rangle]$ must lie parallel to $[S_{n,k}|s\rangle + P_{n,k}|p\rangle]$ which means the right-hand side of (34) is non-zero. The only way it could be zero is if the bands were decoupled in the first place which would mean that effectively a single-band model was being studied. There is in fact an error in [9] which results in the right-hand side of (34) being zero. This is explained in Appendix B.

6. Stark ladders in superlattices

To be able to observe Stark ladders, it has been suggested that a Stark length that is shorter than the sample is required. For instance, to obtain a Stark length that is comparable to the length of the sample being used requires a voltage applied across the sample which is of the order of the band width of the sample measured in electron volts. So for silicon, a voltage greater than ten volts is required. However, to really observe the aperiodic Zener resonances caused by the interaction of Stark ladders in different bands (figure 4), the sample must be shorter than a 'super' Stark length calculated using the valence band, the conduction band and also the gap that separates them, i.e.

$$L > W_1/eF + E_g/eF + W_2/eF \tag{35}$$

where L is the length of the sample, W_1 is the valence band width, E_g the energy gap and W_2 is the conduction band width. To satisfy this equation for most materials would require an unacceptably large field.

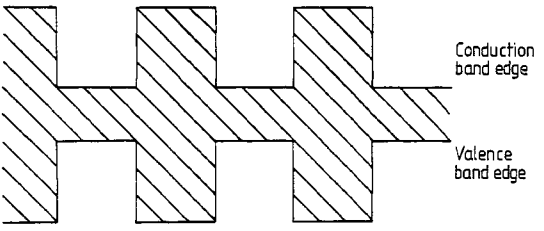

Figure 11. Profile of the band-gap variation that results in the formation of a superlattice. The shaded region represents the band gap.

However, a system in which one could possibly observe the Zener resonances is the semiconductor superlattice which was first proposed by Esaki and Tsu [11] in 1970. Layer-by-layer growth techniques such as molecular beam epitaxy have made it possible to grow layers of material such as GaAs followed by layers of another material such as AlGaAs which has a wider band gap. Repeating this process therefore leads to a structure made up of quantum wells and barriers which can have a lattice constant of anything up to 50 times or more that of the underlying materials (figure 11). The wells will have bound states to confine the electrons and holes and if there is an appropriate overlap between neighbouring wells, minibands can be formed (usually not more than two are formed because the dimensions of the wells only allow two bound states).

In the paper by Esaki and Chang [12], the band widths and gaps were calculated for varying well widths in a AlAs/GaAs superlattice. For a well width of around 45 Å the band width of the valence band was less than 0.01 eV, the band gap was 0.2 eV and the conduction band was 0.04 eV. Therefore if we take all these together we get a total effective band width of 0.25 eV. If the superlattice is say 50 periods long, then to observe Zener tunnelling the Stark length must be less than 4500 Å. This can be obtained with a field strength of $5.5 \times 10^3\,\mathrm{V\,cm^{-1}}$. Also, by varying the well and barrier widths separately, it becomes possible to optimise the band structure for observing the Zener resonances. Namely, to produce narrow bands needed to minimise the Stark length, the barrier widths can be widened, but to regulate the amount of band mixing, the wells widths can be made narrower resulting in a larger band gap.

Movaghar [13] has also studied the role of Stark ladders in superlattices with respect to the transport problem and also discusses the possibility of observing them experimentally. It has already been mentioned in this paper that scattering could broaden the Zener resonances which appear at very low fields to such a degree that their observation could become virtually impossible. We must, however, ensure that this is not the case for all the resonances. There are many possible scattering mechanisms which could result in broadening (for example see [14]) but two of the most likely mechanisms, however, are electron–optic phonon scattering to other Stark states and tunnelling out of the sample and into the contact region. In fact the second of these is essential for any type of current to flow. Therefore, this broadening is unavoidable. For Lorentzian broadening the profile of the resonance is given by

$$\frac{(\Gamma/2)^2}{(E - E_r)^2 + (\Gamma/2)^2} \tag{36}$$

where E_r is the position of the resonance and Γ is the full width at half-maximum and

is given by the lifetime of the Stark–Wannier states. For electron–optic phonon interactions the scattering time is approximately 1×10^{-13} s which results in a Γ_{e-p} of 6 meV. To make an estimate of the rate of tunnelling into the contact region, we assume that it is of the same order of magnitude as the tunnelling rate between bands, therefore $\Gamma_{con} \simeq 2$ meV. These amounts of broadening, therefore, still make it possible to observe at least some of the resonances, especially at high fields when they can be spaced at intervals of about 0.5 eV.

The above theory of Stark ladders and of their possible observation in superlattices assumes that the electric field is uniformly dropped across the whole structure. That means that there are no high-field domains which could result in all or the majority of the field being dropped across one part of the superlattice. This, however, is thought to be what has been observed in many superlattice structures [12, 15, 16, 17] where oscillations in the current are attributed to the movement of a high-field domain through the sample. Therefore, to avoid this happening, one would require a structure similar to that used by Capasso *et al* [18]. In their 35 period superlattice they observe regions of negative differential resistance in the photocurrent which they conclude are not the result of high-field domain formation. This is because their structure is of the type n^+–i–p^+. Therefore, it has a natural built in bias but does not permit the flow of electrons. To obtain a current, a He–Ne laser is used to create electrons as minority carriers in the p^+ layer. The field across the superlattice can then be changed by applying a reverse bias.

Finally, a further aspect involved in the observation of these Zener resonances is the requirement that the electron preserves the phase coherence of its wavefunction across the whole system. That is to say the sample must be of mesoscopic dimensions. However, this requirement can be satisfied fairly simply because of the technology that is now available to produce very pure, high mobility samples.

7. Conclusion

In this paper we have studied a two-band tight-binding model to ascertain how the two bands interact in an electric field. We have demonstrated, using this model, that the matrix elements between the two bands do exist and result in aperiodic oscillations in the Zener tunnelling current. We have also discovered an increase in the Zener current with field which we attribute to the bands getting closer together. An approximate form for this increase was derived showing that the current increases exponentially as minus the reciprocal of the field. The Stark–Wannier wavefunctions for this model were found to be linear combinations of the single band Stark–Wannier wavefunctions, namely Bessel functions of the first kind.

We have also proposed that to observe the aperiodic oscillations in the current produced by the crossing of banded Stark ladders experimentally, a superlattice structure is required. This is because the sample must be longer than a 'super' Stark length which incorporates both energy bands and the gap that separates them and as superlattices have extremely narrow bands, this becomes possible at obtainable electric fields.

Acknowledgments

J Leo would like to thank the Science and Engineering Research Council and GEC

Research for financial support. We would also like to thank Dr B Movaghar for useful discussions.

Appendix 1

To illustrate that (33) is meaningful, consider any periodic function of k. This function can be written as the following Fourier series

$$\sum_{m=-\infty}^{\infty} e^{ikma} C_m. \tag{A1.1}$$

We will now take the derivative of this function with respect to k to give

$$\frac{\partial}{\partial k}\left(\sum_{m=-\infty}^{\infty} e^{ikma} C_m\right) = \sum_{m=-\infty}^{\infty} ima e^{ikma} C_m. \tag{A1.2}$$

As a finite system is being considered, only values of k that are integer multiples of $2\pi/Na$ (where Na is the length of the system) are allowed to be used. Therefore restricting k to these values in (A1.2) and summing over k gives

$$\sum_k \sum_{m=-\infty}^{\infty} ima\, e^{ikma} C_m = \sum_{n=0}^{N-1} \sum_{m=-\infty}^{\infty} ima\, e^{i(2\pi/Na)nma} C_m$$

$$= \sum_{m=-\infty}^{\infty} ima \sum_{n=0}^{N-1} e^{i(2\pi/Na)nma} C_m. \tag{A1.3}$$

The sum over n is the Kronecker delta given in (12). Therefore this term is zero unless $m = 0$. If $m = 0$ then the whole of the right-hand side of (A1.3) is zero. Therefore the sum over k of the derivative of the periodic function is zero, even if k is discrete.

Appendix 2

In the paper by Emin and Hart [9], they showed that the term in the Schrödinger equation that couples different bands under the influence of an electric field results from the alteration of the shape of the potential wells. Our numerical work has shown that this cannot be correct because by using the tight-binding model we neglect any field-dependent alteration of the potential wells and are only considering the step-function potential and still we get band coupling. Using (31) and (34) we also have shown that the only way the bands could possibly be decoupled in our model when there is a field present is if they were decoupled in the unperturbed system. Therefore, there must be a mistake in Emin and Hart's paper that leads them to their conclusion.

From our (34) we have that

$$\delta_{k,k'} \frac{\partial}{\partial k'} I(n, k; n', k')$$

$$= \delta_{k,k'} \int_0^a [\langle s|S^*_{n,k} + \langle p|P^*_{n,k}] \frac{\partial}{\partial k'} [S_{n',k'}|s\rangle + P_{n',k'}|p\rangle] \, dx \tag{A2.1}$$

cannot be zero. In Emin and Hart's paper they prove in the appendix

that this is indeed zero. However, during the proof they make a serious mistake. They are trying to show that the derivative of $\delta_{n,n'}\delta_{k,k'}$ with respect to k' at $k = k'$ is $\delta_{n,n'}\delta_{k,k'}a(N-1)/2$. They do this by writing the two delta functions in terms of Wannier functions. However, they use the orthogonality relation

$$\int_0^{Na} w_n^*(x - pa)w_{n'}(x - p'a)\,\mathrm{d}x = \delta_{n,n'}\delta_{p,p'} \tag{A2.2}$$

where $w(x - pa)$ is the Wannier function centred on $x = pa$ and the integral is over the whole system. However, (A2.2) is incorrect. The Wannier functions are only orthogonal in this way if the integral is from minus infinity to infinity. The problem is that the Wannier functions located at the edge of the system are not orthogonal to the bulk Wannier functions. There is, therefore, an extra surface term which has been neglected in Emin and Hart's paper and which when included no longer results in (A2.1) being zero.

We shall now also calculate the derivative of $\delta_{n,n'}\delta_{k,k'}$ with respect to k' at $k = k'$ and show that in addition to $\delta_{n,n'}\delta_{k,k'}a(N-1)/2$, we obtain the derivative of $I(n, k; n', k')$ with respect to k'. We proceed by replacing the delta functions by two orthogonal Bloch functions.

$$\frac{\partial}{\partial k'}(\delta_{n,n'}\delta_{k,k'})\bigg|_{k=k'} = \frac{\partial}{\partial k'}\left(\frac{1}{N}\int_0^{Na} \mathrm{e}^{\mathrm{i}(k'-k)x}u_{nk}^*(x)u_{n'k'}(x)\,\mathrm{d}x\right)_{k=k'}. \tag{A2.3}$$

These Bloch functions could be the field-dependent type derived in [9]. We then reduce the integral to a unit cell to give

$$\begin{aligned}
&\frac{\partial}{\partial k'}\left(\frac{1}{N}\sum_{p=0}^{N-1}\mathrm{e}^{\mathrm{i}(k'-k)pa}\int_0^a \mathrm{e}^{\mathrm{i}(k'-k)x}u_{nk}^*(x)u_{n'k'}(x)\,\mathrm{d}x\right)_{k=k'} \\
&\quad = \frac{1}{N}\sum_{p=0}^{N-1}\mathrm{i}ap\,\mathrm{e}^{\mathrm{i}(k'-k)pa}\int_0^a \mathrm{e}^{\mathrm{i}(k'-k)x}u_{nk}^*(x)u_{n'k'}(x)\,\mathrm{d}x\bigg|_{k=k'} \\
&\qquad + \frac{1}{N}\sum_{p=0}^{N-1}\mathrm{e}^{\mathrm{i}(k'-k)pa}\frac{\partial}{\partial k'}\int_0^a \mathrm{e}^{\mathrm{i}(k'-k)x}u_{nk}^*(x)u_{n'k'}(x)\,\mathrm{d}x\bigg|_{k=k'} \\
&\quad = \frac{1}{N}\sum_{p=0}^{N-1}\mathrm{i}ap\int_o^a u_{nk}^*(x)u_{n'k}(x)\,\mathrm{d}x + \delta_{k,k'}\frac{\partial}{\partial k'}\int_0^a \mathrm{e}^{\mathrm{i}(k'-k)x}u_{nk}^*(x)u_{n'k'}(x)\,\mathrm{d}x \\
&\quad = \frac{(N-1)}{2}\mathrm{i}a\delta_{n,n'}\delta_{k,k'} + \delta_{k,k'}\frac{\partial}{\partial k'}I(n, k; n', k').
\end{aligned} \tag{A2.4}$$

Therefore we have now regained the extra term that was absent in Emin and Hart's result. Also note that the second term in (A2.4) cannot be simply cancelled in the limit N goes to infinity even though it is a surface term. In the next step in Emin and Hart's argument another quantity is calculated which involves the same term of order $(N-1)$ as is in (A2.4). These terms are then subtracted to yield a result of order unity. Therefore, the limit of N tending to infinity has to be taken after this subtraction to leave a term of finite magnitude.

References

[1] Zener C 1934 *Proc. R. Soc.* A **145** 523
[2] Wannier G H 1954 *Elements of Solid State Theory* (London: Cambridge University Press) pp 190–3
[3] Wannier G H 1960 *Phys. Rev.* **117** 432
[4] Saitoh M 1972 *J. Phys. C: Solid State Phys.* **5** 914
[5] Wannier G H 1956 *Phys. Rev.* **101** 1835
[6] Wannier G H 1955 *Phys. Rev.* **100** 1227
[7] Kane E O 1959 *J. Phys. Chem. Solids* **12** 181
[8] Fukuyama H, Bari R A and Fogedby H C 1973 *Phys. Rev.* B **8** 5579
[9] Emin D and Hart C F 1987 *Phys. Rev.* B **36** 7353
[10] Bell R J and Dean P 1971 *Discuss. Faraday Soc.* **50** 51
[11] Esaki L and Tsu R 1970 *IBM J. Res. Dev.* **14** 61
[12] Esaki L and Chang L 1974 *Phys. Rev. Lett.* **33** 495
[13] Movaghar B 1987 *Semicond. Sci. Technol.* **2** 185
[14] Movaghar B, Leo J and MacKinnon A 1988 *Semicond. Sci. Technol.* **3** 397
[15] Kawamura Y, Wakita K, Asahi H and Kurumada K 1986 *Japan. J. Appl. Phys.* **25** L928
[16] Choi K K, Levine B F, Malik R J, Walker J and Bethea C G 1987 *Phys. Rev.* B **35** 4172
[17] Vuong T H H, Tsui D C and Tsang W T 1988 *Appl. Phys. Lett.* **52** 981
[18] Capasso F, Mohammed K and Cho A Y 1986 *Appl. Phys. Lett.* **48** 478